Calcified Tissue International (2022) 110:93–103
https://doi.org/10.1007/s00223-021-00888-3

ORIGINAL RESEARCH

Fibroblast Growth Factor 2 High Molecular Weight Isoforms in Dentoalveolar Mineralization

Grethel Millington[1] · Johnny Joseph[4] · Liping Xiao[3] · Anushree Vijaykumar[2] · Mina Mina[2] · Marja M. Hurley[3]

Received: 21 October 2020 / Accepted: 2 July 2021 / Published online: 10 July 2021

Abstract

Transgenic mice overexpressing human high molecular weight fibroblast growth factor 2 (HMWFGF2) isoforms in osteoblast and odontoblast lineages (HMWTg) exhibit decreased dentin and alveolar bone mineralization, enlarged pulp chamber, and increased fibroblast growth factor 23 (FGF23). We examined if the alveolar bone and dentin mineralization defects in HMWTg mice resulted from increased FGF23 expression and whether an FGF23 neutralizing antibody could rescue the hypomineralization phenotype. HMWTg and VectorTg control mice were given subcutaneous injections of FGF23 neutralizing antibody twice/week starting at postnatal day 21 for 6 weeks. Since Calcitriol (1,25D) have direct effects in promoting bone mineralization, we also determined if 1,25D protects against the defective dentin and alveolar bone mineralization. Therefore, HMWTg mice were given subcutaneous injections of 1,25D daily or concomitantly with FGF23 neutralizing antibody for 6 weeks. Our results showed that HMWTg mice displayed thickened predentin, alveolar bone hypomineralization, and enlarged pulp chambers. FGF23 neutralizing antibody and 1,25D monotherapy partially rescued the dentin mineralization defects and the enlarged pulp chamber phenotype in HMWTg mice. 1,25D alone was not sufficient to rescue the alveolar bone hypomineralization. Interestingly, HMWTg mice treated with both FGF23 neutralizing antibody and 1.25D further rescued the enlarged pulp chamber size, and dentin and alveolar bone mineralization defects. We conclude that the dentin and alveolar bone mineralization defects in HMWTg mice might result from increased FGF23 expression. Our results show a novel role of HMWFGF2 on dentoalveolar mineralization.

Keywords Dentin · Odontoblast(s) · Osteoblast(s) · Mineralized tissue · Development · Fibroblast growth factor 2 · Hypophosphatemia

Introduction

Fibroblast growth factor 2 (FGF2), a member of the FGF family of ligands, is mitogenic for osteoblasts, induces early differentiation of odontoblasts, and is critical for regulating bone matrix mineralization [1–4]. A single Fgf2 gene encodes multiple FGF2 isoforms, an exported low molecular weight isoform, and several high molecular weight (HMW) isoforms. HMWFGF2 isoforms are nuclear localized and function in an intracrine manner to regulate the expression of target genes [5–8], however, the biological functions of HMWFGF2 isoforms are not fully defined.

XLH is caused by loss-of-function mutations in phosphate-regulating gene with homologies to endopeptidases on the X chromosome (*PHEX*) [9] and the Hyp mouse homolog phenocopies the human disease. Of importance for the current study, the expression of both HMWFGF2 and FGF23 is elevated in the Hyp mouse [10]. In addition, we reported

✉ Grethel Millington
millington.grethel@gmail.com

✉ Marja M. Hurley
hurley@uchc.edu

1 University of Connecticut School of Dental Medicine, Farmington, CT, USA

2 Department of Craniofacial Sciences, University of Connecticut School of Dental Medicine, Farmington, CT, USA

3 Department of Medicine, University of Connecticut School of Medicine, UConn Health, Farmington, CT 06030-052, USA

4 NYU Langone Health, Postdoctoral Pediatric Dentistry Program, Brooklyn, NY 11220, USA

that transgenic mice overexpressing the human HMWFGF2 (24 kDa, 23 kDa, and 22 kDa) isoforms in osteoblast and odontoblast lineages using the Col3.6 promoter (HMWTg) phenocopies the Hyp mouse and XLH subjects. HMWTg mice presents with reduced bone mineral density (BMD), osteomalacia, hypophosphatemia, and increased FGF23 in serum and bone [10].

In the disease XLH, PHEX functions to inactivate FGF23 through its metalloprotease activity [11]. Loss-of-function *PHEX* mutations result in elevated FGF23 hormone levels and impaired renal production of 1,25-dihydroxyvitamin D (1,25D) and inorganic phosphate (P_i) reabsorption [12–15]. The increased FGF23 activity in XLH inhibits renal phosphate reabsorption in the proximal renal tubules, thereby promoting excessive P_i urine excretion [16, 17]. Renal P_i reabsorption is required for many biological systems including dentinogenesis, the process of dentin formation within the tooth. Dentin matrix is secreted by odontoblasts as unmineralized predentin that is converted to mineralized dentin, in a process that requires both Ca and P_i deposition [17]. The major oral manifestations of XLH include spontaneous dental abscesses affecting non-carious primary and permanent teeth, which exhibit high pulp horns, large pulp chambers, and dysplastic and poorly mineralized dentin [18–21].

Although FGF23 is known to play a major role in the pathogenesis of hypophosphatemia and the associated appendicular bone hypomineralization in XLH, the cause of the dentoalveolar hypomineralization in XLH is not fully understood. This study explores the role of HMWFGF2 and FGF23 in dentoalveolar mineralization in HMWTg mice.

Materials and Methods

Mice

The UConn Health Institute of Animal Care and Use Committee approved animal protocols. Generation of Col3.6-HMWFgf2 isoform-IRES-GFPsaph mice on FVBN background was previously described in detail [10]. Generation of Col3.6-IRES/GFPsaph (VectorTg) mice which were used as controls was also previously described in detail (10). In brief, Col3.6-HMWFgf2 isoforms-IRES-GFPsaph (Green Fluorescent Protein- Sapphire) was built by replacing a chloramphenicol acetyltransferase fragment in previously made Col3.6-CAT-IRES-GFPsaph with HMW isoforms of human Fgf2 cDNA. This expression vector concurrently overexpresses HMW and GFPsaph from a single bicistronic mRNA. Col3.6-IRES/GFPsaph (Vector) construct was also prepared as a control. The construct inserts were released from Col3.6-IRES/GFP (Vector) or Col3.6-HMWFgf2 isoforms-IRES-GFPsaph by digestion with AseI and AflII. Microinjections into the pronuclei of fertilized oocytes were performed at the Gene Targeting and Transgenic Facility at the University of Connecticut Health Center. Founder mice of the F2 (FVBN) strain were bred with wild-type mice to establish individual transgenic lines. Mating of heterozygote male and female generated homozygote mice that were used in this study. Mice were euthanized for sample collection at 60 d of postnatal unless stated otherwise. Female and male mice were used in this study.

FGF23 Neutralizing Antibody (FGF23Ab) and Calcitriol Treatment

FGF23Ab (Amgen Inc., Thousand Oaks, CA) or IgG (rat-anti-NGFPb-3F8-raIgG2a) was administered. Subcutaneous (sc) injections of FGF23Ab (10 mg/kg, twice/week) or/and Calcitriol (175 pg/g, daily) were given starting at 21-dpn for 6 weeks. Dosage and interval were based on published protocols [22, 23]. For these studies "the vehicle group" refers to IgG for FGF23 antibody treatment, while it refers to water in Calcitriol treatment. Mice were euthanized after 6 weeks by carbon dioxide for sample collection with 8 female mice per treatment group.

Radiography

Radiographs of hemisected mandibles were taken using CABINET X-RAY SYSTEM (Faxitron X-Ray Corporation, Lincolshire, IL) at 25 kV, 20-s exposure at 4.5X magnification.

Micro-computed Tomography

60-dpn mandibles were used for analysis with micro-CT with 3 mice per group. µCT40, Scanco Medical (Bassersdorf, Switzerland) system was used for acquisition, data analysis, and 3D reconstruction, and calibrated using a phantom provided by the manufacturer. Samples were scanned in 70% ethanol at high resolution (6 microns) with an energy level of 55 kVp, intensity of 145 µA, and integration time of 300 ms. 3D analysis was conducted from 2D scanned slices to calculate morphometric parameters defining microarchitecture, including pulp chamber volume, alveolar bone volume fraction (BVF), and apparent density.

Histology

Hematoxylin and eosin (H&E) immunohistochemistry experiments were performed on decalcified mandibles per standard protocols with anti-FGF23 (R&D SYSTEMS, MAB26291) at 1:50 dilution. von Kossa staining was completed on formalin-fixed undecalcified mandibles embedded in Cryomatrix per standard protocols. 7-µm coronal sections

were collected on Cryofilm type IIC (FINETEC Co. Ltd., Japan) cold adhesive tape. Images were captured with Nikon E400 microscope (Nikon Inc., Melville, NY). Alveolar BA/TA% measurements were completed non-biased and blinded using OsteoMeasure image analysis (R&M Biometrics, Nashville, TN, USA).

Calcium, Phosphate, and PTH Serum Biochemistry

Blood was collected from euthanized animals by cardiac puncture. Serum phosphate and calcium were measured using Phosphorus Liqui-UV (StanBio Laboratory, Boerne, TX) and calcium reagent SET (Eagle Diagnostics, Cedar Hill, TX), respectively. Serum PTH was determined using mouse intact PTH ELISA kit (Immunotopics, Athens, OH).

Statistical Analysis

Results are presented as means ± SEM. Normal distribution was evaluated with the Shapiro–Wilk normality test. Samples were normally distributed. Student's t-test and one-way ANOVA with LSD post hoc follow-up test were used to analyze differences between treatment groups. Differences were considered significant at $P < 0.05$. Sample size and power calculation were based on the effect size and standard deviation of the serum Pi in Vector and HMW obtained from our published data with a difference of 3.5 mg/dL in serum Pi between Vector and HMW, and standard deviation of 2.6 mg/dL. The minimal sample size necessary determined was $n = 3$.

Results

Aberrant Dentin Mineralization and Enlarged Pulp Chamber in HMWTg Mice

We previously characterized the long bone mineralization defects in HMWTg mice. Further examination of these mutants revealed abnormalities in dentoalveolar mineralization. To understand the basis of these abnormalities, we characterized the dental phenotype in HMWTg mice. H&E-stained coronal sections through 60-dpn mandibular first molars revealed thin mineralized dentin and an expanded unmineralized predentin in HMWTg mice (Fig. 1A–D). The total dentin and mineralized dentin were significantly thinner in HMWTg mice with thicker predentin (Fig. 1E–F). Micro-CT analysis of 60-dpn male and female mandibular first molars showed enlarged pulp chamber in HMWTg mice (Fig. 1G–J). 3D volumetric reconstruction of the pulp chamber further illustrates markedly enlarged coronal pulp and radicular pulp chambers in male and female HMWTg molars (Fig. 1K–N). We quantified the coronal pulp and the total pulp chamber volumes. The floor of the pulp chamber was employed as a reliable landmark to demarcate coronal pulp from radicular pulp canals. In both male and female HMWTg mandibular first molars, a significant increase in the coronal and total pulp chamber volume was observed (Fig. 1O–R). Together, these results indicate that mice overexpressing HMWFGF2 in odontoblast and osteoblast lineages exhibit thinner dentin, thicker predentin layers, and enlarged pulp volume.

Aberrant Alveolar Bone Mineralization in HMWTg Mice

To examine the alveolar bone morphology in HMWTg mandibles, we analyzed the alveolar bone in 60-dpn male and female mice using Micro-CT. 3D images revealed large marrow spaces in the alveolar bone of both male and female HMWTg mice compared with VectorTg control (Fig. 2A-D). Transverse Micro-CT images at the furcation of mandibular first molars revealed large marrow spaces and markedly reduced radiodense regions in both male and female HMWTg mandibles (Fig. 2E–H). Quantification of the alveolar bone revealed a significant reduction in alveolar BVF between VectorTg and HMWTg groups (Fig. 2I–J). In addition, the apparent density was significantly decreased in both male and female HMWTg mice (Fig. 2K–L). Alveolar bone mineralization was examined by von Kossa staining, which was localized to dentin and alveolar bone in both VectorTg and HMWTg (Fig. 2M–N). However, less von Kossa staining was detected in the alveolar bone of HMWTg mandibles (Fig. 2O–P). The reduced von Kossa staining is consistent with decreased BVF and apparent density and together indicates decreased alveolar bone mineralization in HMWTg mice.

FGF23 Neutralizing Antibody Reduces FGF23 Expression in HMWTg Mice

We previously reported that serum FGF23 is elevated in HMWTg mice [10]. We performed immunohistochemistry to analyze FGF23 expression in mandibles of HMWTg. FGF23 expression was evident in odontoblasts, alveolar bone, and periodontal ligament of VectorTg and HMWTg mandibles (Fig. 3A–B). A magnified view of the odontoblasts lining the pulp cavity showed increased FGF23-positive odontoblasts in HMWTg mice. FGF23 staining was absent in the predentin and dentin (Fig. 3A'–B, arrow). A magnified view of the alveolar bone showed elevated FGF23 expression in the marrow spaces and the trabeculated alveolar bone (Fig. 3A"–B").

Our previous work showed that FGF23Ab significantly increased BMD in femurs of HMWTg mice [24]. We next determined whether FGF23Ab reduces FGF23

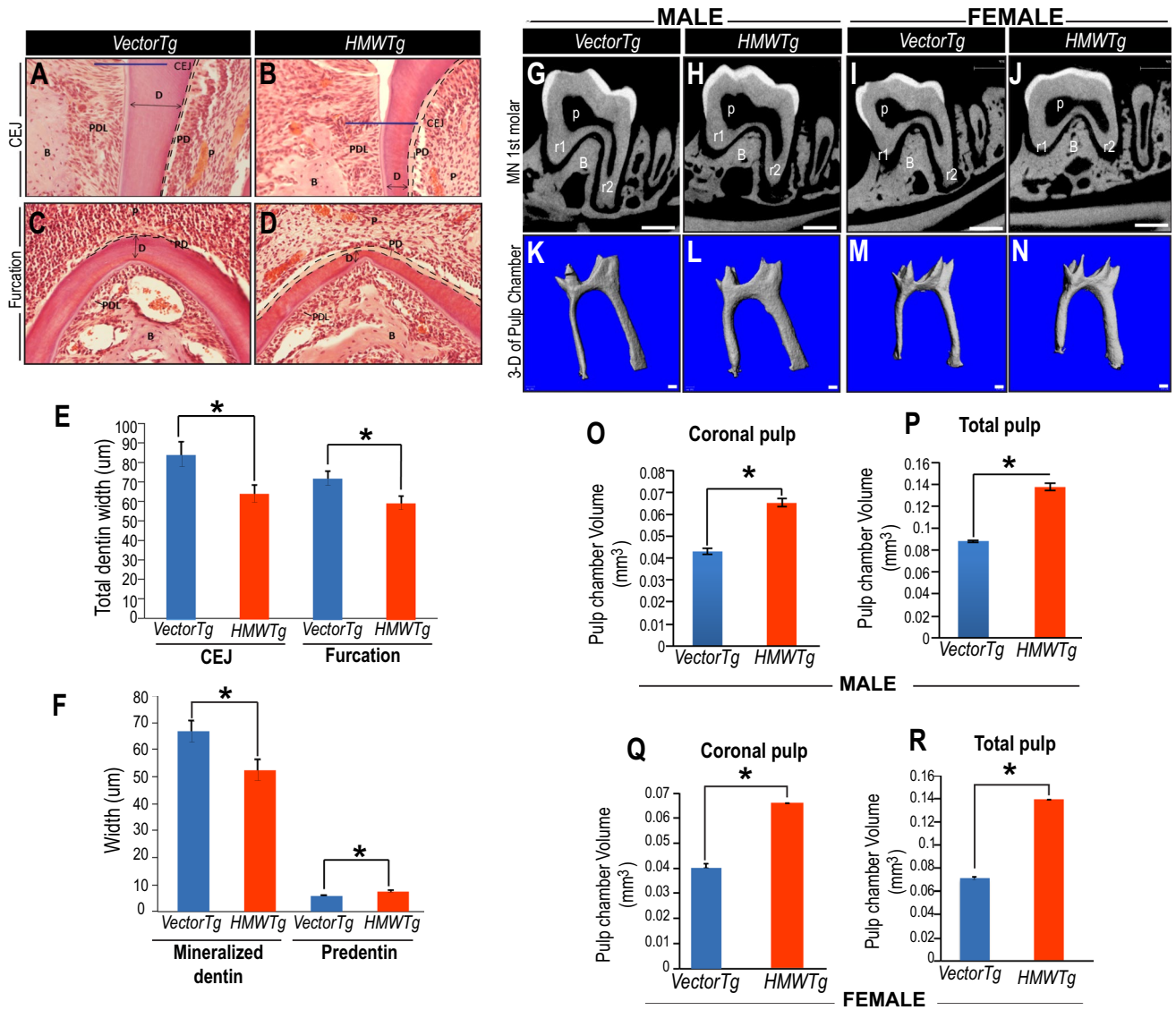

Fig. 1 Defective dentin mineralization and enlarged pulp chamber in HMWTg mice. H&E staining of coronal sections of 60-dpn mandibular molar tooth from Vector and HMWTg male mice. Thickness of dentin (double head arrows) and predentin (dotted lines) examined at cemento-enamel junction (CEJ) and furcation (A-D; blue horizontal line denotes the CEJ). Images were acquired at 20X magnification. (E) Quantification of total dentin thickness (includes both mineralized and predentin) at CEJ and furcation ($p < 0.05$; $n = 4$). (F) Comparison of dentin and predentin thickness at furcation in HMWTg mice compared to VectorTg controls ($p < 0.05$; $n = 4$). Coronal view of Micro-CT images from 60-dpn male (G-H) and female (I-J) mandibular molar. Micro-CT 3D representation of pulp chamber in male (K-L) and female (M–N) molar teeth in VectorTg and HMWTg mice. (O-R) Coronal and total pulp chamber quantification in male and female VectorTg and HMWTg mice ($P < 0.05$; $n = 3$). Scale bar = 500um. P: pulp chamber; B: alveolar bone; D: dentin; PD: predentin; r1: mesial root; r2: distal root, PDL: periodontal ligament; B: alveolar bone; MN: mandible. Student's T test was utilized for statistical analysis

expression in HMWTg mandibles. Mandibles of HMWTg mice treated with FGF23Ab showed a marked reduction in FGF23 staining in the odontoblast and alveolar bone (Fig. 3C–C"). Quantification of the FGF23 immunohistochemistry showed that FGF23 (+) odontoblast and osteocytes were significantly elevated in HMWTg mandibles which was significantly reduced with FGF23Ab treatment (Fig. 3D–E). Together, Our findings demonstrated that FGF23 protein is increased in odontoblasts and alveolar bone of HMWTg mice and FGF23Ab treatment reduces the FGF23 immunostaining odontoblast and osteocytes in HMWTg mandibles.

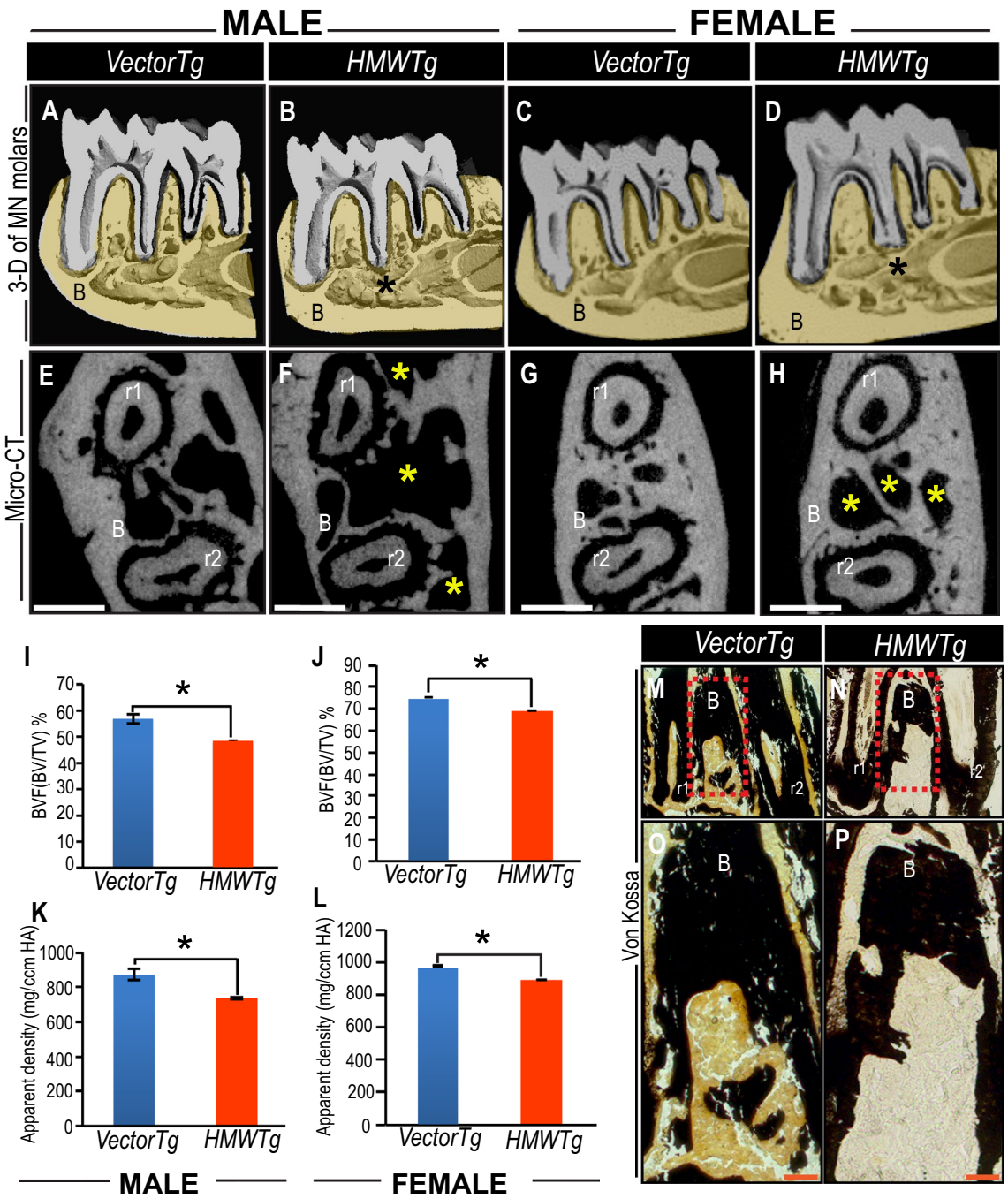

Fig. 2 Defective alveolar bone mineralization in HMWTg mice. 3D Micro-CT representation of alveolar bone in male (A, B) and female (C, D) VectorTg and HMWTg mandibles. Axial view of Micro-CT analysis on 60-dpn mandibular molars from male (E–F) and female (G-H) VectorTg and HMWTg mice. (*) show areas of larger bone marrow spaces in HMWTg mandibles. Quantification of bone volume fraction (BVF) and apparent bone density in male and female VectorTg and HMWTg mandibles (I-L) ($p < 0.05$; $n = 3$). von Kossa mineral staining on coronal sections of 60-dpn VectorTg and HMWTg mandibular molars (M-P). Scale bar (E–H) = 500um; Scale bar (M-P) = 100um. B: alveolar bone; r1: mesial root; r2: distal root; MN: mandible. Student's T test was utilized for statistical analysis

FGF23 Neutralizing Antibody Rescues Dentin Hypomineralization in HMWTg Mice

We previously reported that FGF23Ab rescued hypophosphatemia and osteomalacic bone phenotype of HMWTg mice [24]. We performed H&E staining to examine the effects of FGF23Ab on the increased predentin phenotype in HMWTg mice. HMWTg mice treated

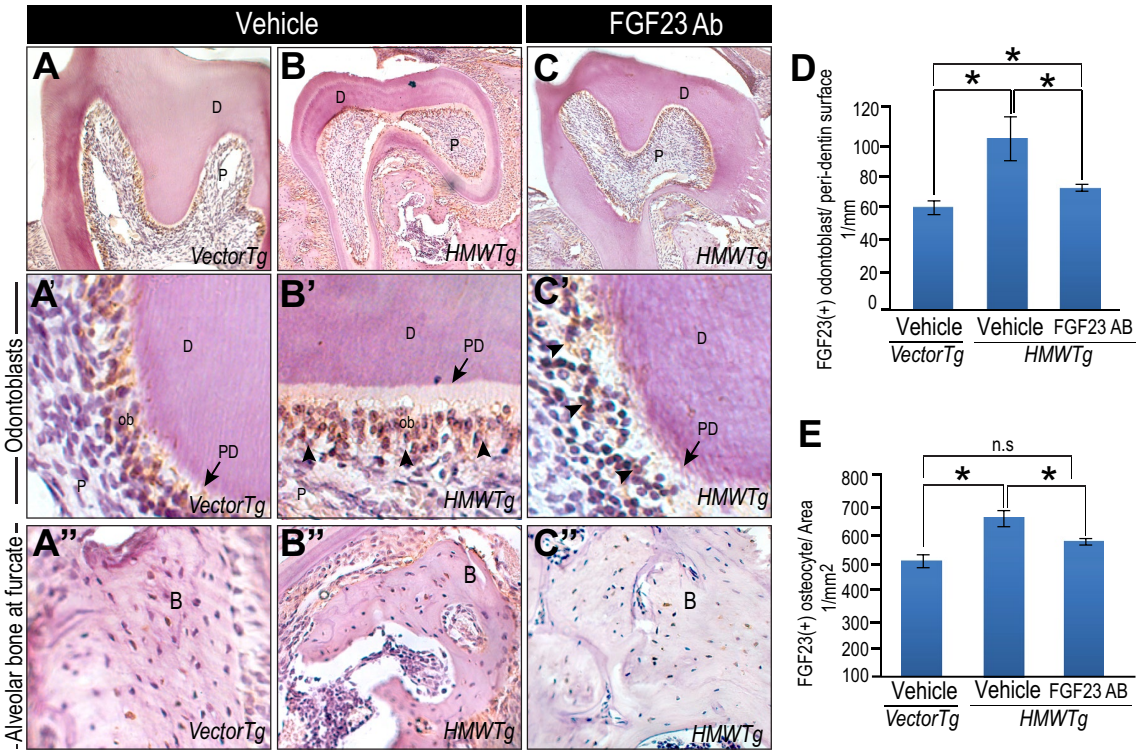

Fig. 3 FGF23 Neutralizing antibody decreases FGF23 immunostaining in HMWTg mice. (A–B) FGF23 immunohistochemistry on coronal sections through mandibular molars in VectorTg and HMWTg mice treated with IgG as the vehicle group. Images are taken at 10X magnification. Compared to VectorTg mice, FGF23 expression is increased in the odontoblast (A'–B') and alveolar bone (A"–B") of HMWTg control mice. (C) FGF23 immunohistochemistry on sagittal sections through mandibular molars of HMWTg mice treated with FGF23 neutralizing antibody. Images are taken at 10X magnification. FGF23 expression is reduced in the odontoblast (C') and alveolar bone (C") of HMWTg mice treated with FGF23 neutralizing antibody. Images were taken at 20X magnification. (D–E) Quantification of FGF23 immunohistochemistry. FGF23 (+) odontoblasts and osteocytes increased in HMWTg mice which were reduced with FGF23 neutralizing antibody treatment. *$p < 0.05$; $n = 7$. n.s: not significant; PD: predentin; D: dentin; ob: odontoblasts; B: alveolar bone

FGF23Ab which showed a marked decrease in predentin thickness that was comparable to vehicle VectorTg control groups (Fig. 4A–C). These findings suggest that FGF23Ab treatment rescued the widened predentin in HMWTg mice.

We compared the predentin phenotype of HMWTg mice that were given sc injections of 1,25D with vehicle HMWTg mice to determine if 1,25D supplementation could rescue the dentin hypomineralization. H&E staining showed decreased predentin thickness in HMWTg-1,25D group that was comparable to vehicle VectorTg molars (Fig. 4D). Furthermore, we asked whether a combination of FGF23Ab and 1,25D has enhanced effects on improving dentin mineralization than FGF23Ab or 1,25D monotherapy. H&E-stained coronal sections at the furcation of mandibular first molar showed marked decrease in predentin thickness in HMWTg-FGF23Ab and 1,25D group that was comparable to vehicle VectorTg molars (Fig. 4E).

Taken together, these results suggest that FGF23Ab treatment rescued the widened predentin phenotype of HMWTg mice. We also demonstrated that 1,25D alone or in combination with FGF23Ab were sufficient to decrease predentin thickness in HMWTg mice.

FGF23 Neutralizing Antibody in Combination with 1,25D Improves Alveolar Bone Morphology in HMWTg Mice

To determine if FGF23Ab treatment improves alveolar bone morphology in HMWTg mice, we compared the alveolar bone morphology of vehicle controls with HMWTg mice that were treated with FGF23Ab. We observed less marrow spaces in the alveolar bone of HMWTg were given FGF23Ab treatment as compared to vehicle groups (Fig. 4F–H). These findings were consistent among numerous serial sections analyzed per sample. We observed a partial improvement of the alveolar bone morphology with FGF23Ab treatment. We asked if 1,25D alone or in combination of FGF23Ab improves the alveolar bone morphology in HMWTg mice. In HMWTg-1,25D group, we observed that the alveolar bone

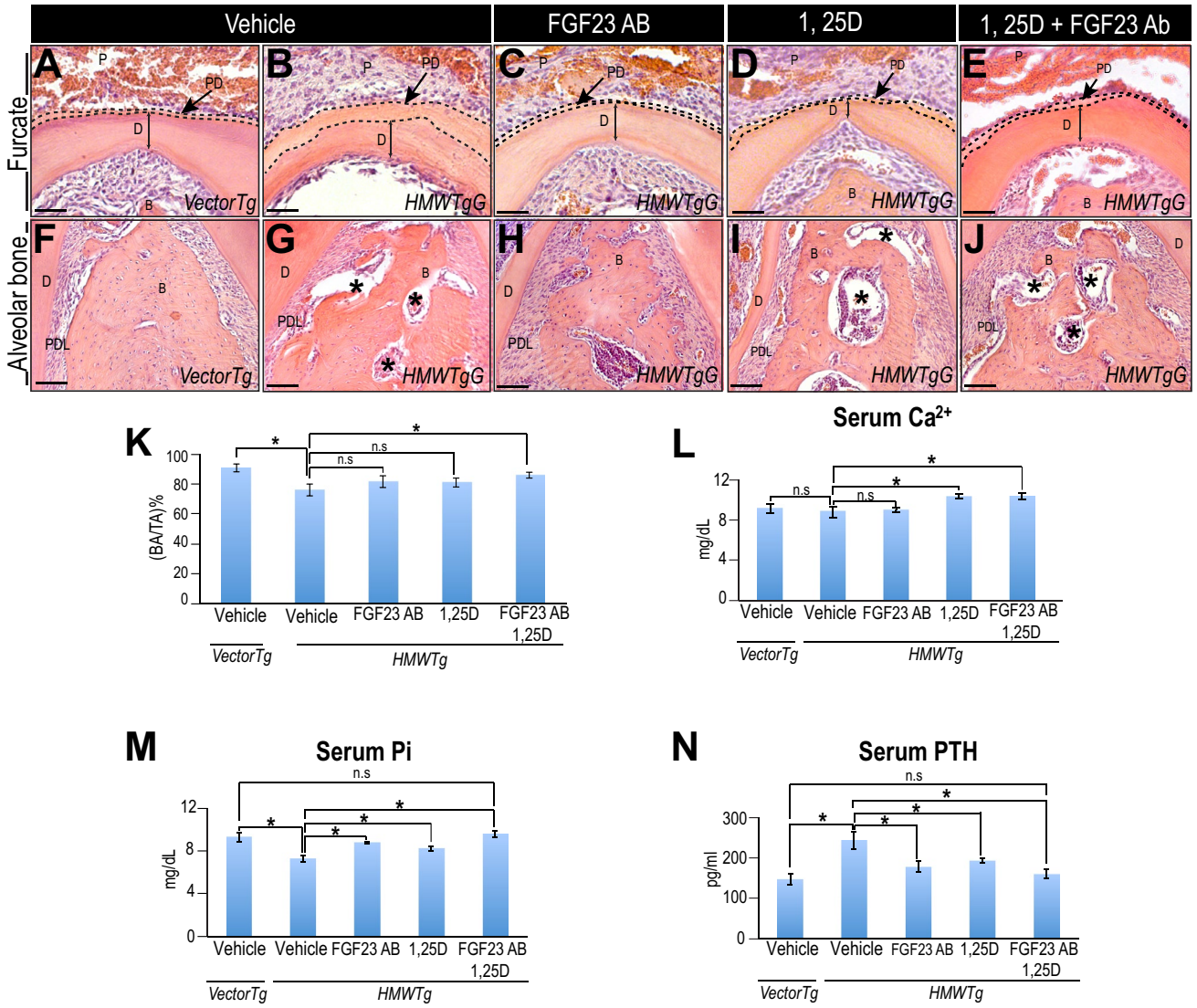

Fig. 4 Effect of FGF23 neutralizing antibody and 1,25D on dentin and alveolar bone morphology in HMWTg mice. H&E staining from coronal sections of vehicle (IgG for FGF23 antibody treatment and water in Calcitriol treatment) treated with VectorTg and HMWTg mice. Representative image were taken at the furcation (A–B). HMWTg mice treated with FGF23 neutralizing antibody shows a reduction in predentin width (C; dotted lines). H&E staining at the furcation of mandibular first molars treated with 1,25D showed reduction in predentin width (D; dotted lines). HMWTg mice treated with both 1,25D and FGF23 neutralizing antibody shows decreased predentin width (F; dotted lines). H&E staining from vehicle treated with VectorTg and HMWTg comparing alveolar bone morphology (F–G; asterisk (*) in G depicts large marrow spaces). Alveolar bone of HMWTg mice treated with FGF23 neutralizing antibody is partially comparable to VectorTg mandibles (H). 1,25D had no observable effect on rescuing the alveolar bone mineralization defects in HMWTg mice (I; asterisk (*) depicts large marrow spaces). Alveolar bone morphology of HMWTg mice that were treated with both Calcitriol and FGF23 neutralizing antibody (J; asterisk (*) depicts large marrow spaces). Quantification of alveolar bone BA/TA%, (K) (n = 3–5: $p < 0.05$). Quantitation of serum calcium, phosphate, and PTH (L–N) (n = 8; $p < 0.05$). One-way ANOVA was utilized for statistical analysis. Scale bar = 50um; PD: predentin; D: dentin; B: alveolar bone; PDL: periodontal ligament

was narrow with large marrow spaces (Fig. 4I). Conversely, HMWTg mice treated with both FGF23Ab and 1,25D exhibited wider alveolar bone and reduced marrow spaces when compared with HMWTg-vehicle mandibles (Fig. 4J). Although we observed marked morphological improvements in alveolar bone of HMWTg mice treated with FGF23Ab or 1,25D, quantification of alveolar BA/TA% by histomorphometry revealed no significant differences between FGF23Ab or 1,25D treatment monotherapy compared to HMWTg-vehicle mandibles. However, combined FGF23 and 1,25D treatment significantly increased alveolar BA/TA% in HMWTg mice (Fig. 4K).

Calcium, P_i, and parathyroid hormone (PTH) directly influences dentoalveolar mineralization [25]. We measured serum levels of calcium, P_i, and PTH in HMWTg mice in each treatment group. We observed no significant differences in serum calcium in HMWTg mice with IgG or FGF23Ab treatment when compared with VectorTg-vehicle group. 1,25D alone or concurrent with FGF23Ab showed a significant increase in serum calcium levels (Fig. 4L). Serum P_i was decreased in HMWTg-vehicle group and FGF23Ab or 1,25D single treatment increased serum phosphate levels. Furthermore, combined FGF23Ab and 1,25D treatment increased serum P_i to VectorTg-vehicle levels (Fig. 4M). Additionally, serum PTH was elevated in HMWTg-vehicle mice compared with VectorTg-vehicle controls. FGF23Ab or 1,25D treatment decreased serum PTH in HMWTg mice. Furthermore, serum PTH levels were reduced to VectorTg-vehicle levels in HMWTg mice with FGF23 and 1,25D combined treatment (Fig. 4N).

Taken together, FGF23Ab in combination with 1,25D improved alveolar bone morphology, increases alveolar BA/TA%, and restored serum P_i and PTH to normal levels in HMWTg mice.

FGF23 Neutralizing Antibody Rescues Enlarged Pulp Chamber Phenotype in HMWTg Mice

We next asked whether neutralizing FGF23 rescues the increased pulp chamber size in HMWTg mice. Radiograph of hemisected mandibles showed decreased radiopacity in mandibles and molars from HMWTg-vehicle mice compared with VectorTg-vehicle controls (Fig. 5A–B). A magnified view showed high pulp horns and large coronal pulp chamber in HMWTg-vehicle molar teeth (Fig. 5A'–B'). HMWTg-FGF23Ab group showed increased radiopacity

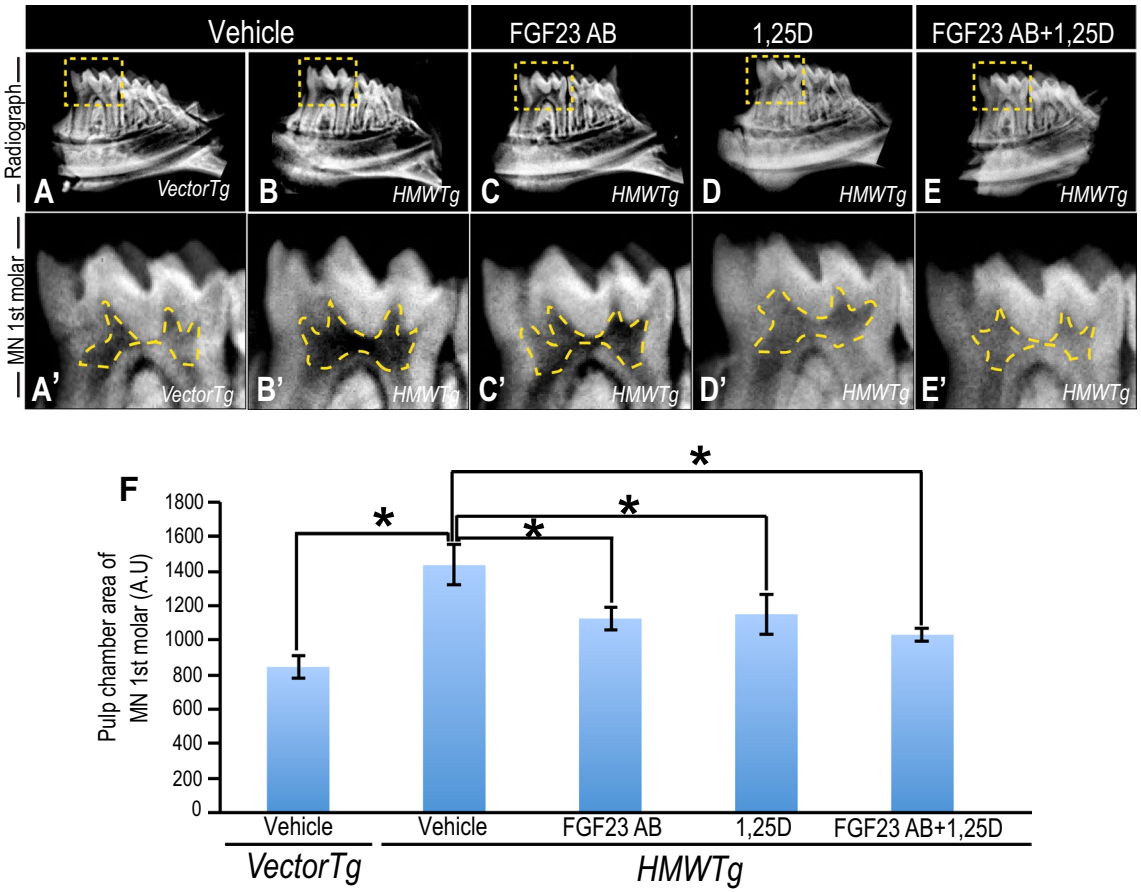

Fig. 5 FGF23 neutralizing antibody rescues the enlarged pulp chamber phenotype in HMWTg mice. Radiograph of vehicle treated VectorTg and HMWTg hemisected mandible (A–B). Magnified radiograph of mandibular first molar (yellow dotted line outlines the coronal pulp chamber) illustrates enlarged pulp chamber in HMWTg molars (A'–B'). The pulp chamber size is decreased in HMWTg mice treated with FGF23 neutralizing antibody and Calcitriol (C–C' and D–D'). HMWTg mice treated with both 1,25D and FGF23 neutralizing antibody further reduces the pulp chamber size (E–E'). Quantification of pulp chamber area in VectorTg and HMWTg molars (F) $p < 0.05$; $n = 5$. n.s: not significant; $n = 6$. MN: mandible. One-way ANOVA utilized for statistical analysis

in mandibles and reduced pulp chamber size (Fig. 5C–C'). In HMWTg-1,25D group, we observed increased mandibular radiopacity (Fig. 5D) and examination of the pulp chamber revealed reduced pulp chamber size (Fig. 5D'). With FGF23Ab and 1,25D treatment in HMWTg mice, we observed increased alveolar bone radiopacity, and reduced pulp chamber size (Fig. 5E–E').

To determine whether the observed changes were statistically significant, coronal pulp chambers were quantified using ImageJ. There was a significant increase in pulp chamber size in HMWTg-vehicle-treated mice relative to VectorTg-vehicle group. HMWTg-FGF23Ab group showed a significant reduction in coronal pulp chamber area when compared with HMWTg-vehicle group. HMWTg mice treated with 1,25D alone resulted in a significant decrease in pulp chamber; however, pulp chamber size was further reduced when combined with FGF23Ab treatment (Fig. 5F).

Together, we showed that FGF23Ab monotherapy rescued the enlarged pulp chamber in HMWTg mice; however, in combination with 1,25D, the pulp chambers were similar to VectorTg mice.

Discussion

Transgenic mice overexpressing hHMWFGF2 isoforms in osteoblast and odontoblast lineages are characterized by hypomineralized dentin and alveolar bone, and enlarged pulp chamber. We determined that the dentoalveolar mineralization defects and enlarged pulp chamber of HMWTg mice could be attributed in part to increased FGF23 signaling and are partially rescued by FGF23Ab treatment.

The dentoalveolar defects in Hyp mice are well established [26, 27]. We reported that Hyp mice overexpress HMWFGF2 in osteoblasts [10]. Our observations including increased predentin, decreased dentin, enlarged pulp, and hypomineralized alveolar bone in HMWTg mice are consistent with the studies by Fong et al. that showed similar defects in Hyp mice [27]. The increase in unmineralized predentin at the expense of mineralized dentin in HMWTg molar teeth suggests that HMWFGF2 does not impede odontoblast differentiation and the production of predentin matrix but diminishes the mineralization of predentin to form dentin. Odontoblasts secrete predentin that is equivalent to the osteoid layer in osteogenesis [25]. Like osteoid, mineralization of predentin is dependent upon extracellular matrix proteins and minerals such as calcium and P_i [17]. Overexpressing HMWFGF2 decreases serum phosphate. One mechanism is by decreasing renal phosphate reuptake by downregulating the sodium-dependent phosphate transport protein 2A (NPT2A), resulting in hypophosphatemia and osteomalacia [10]. Of relevance we previously published [28] that the kidney phenotype included significantly decreased the phosphate transporter Npt2a mRNA and protein in HMWTg mice that was rescued by in vivo FGF23AB treatment**.** Therefore, the dentin and alveolar bone mineralization defects are partly due to reduced NPT2A resulting in phosphate wasting in HMWTg mice. The phosphaturic factor FGF23 mediates the P_i wasting of XLH [10, 22]. Renal phosphate excretion is significantly increased in HMWTg mice [24]. The osteomalacia of the appendicular bones and P_i wasting phenotypes of HMWTg mice is partially due to elevated FGF23/FGFR signaling [10]. HMWFGF2 isoforms transcriptionally regulate FGF23, which leads to elevated FGF23 in serum and bone [10, 29]. Our findings in HMWTg mandibles showed elevated FGF23 expression localized to the odontoblasts, periodontal ligament, and the alveolar bone. Since FGF23Ab only partially rescues the mineralization defects, elevation of both results in dentoalveolar mineralization defects. Thus, HMWFGF2 and FGF23 both play a role to inhibit proper dentoalveolar mineralization.

The dentoalveolar phenotype of HMWTg mice parallels other genetic hypophosphatemic murine models with elevated serum and local FGF23. Transgenic mice with DMP1 (dentin matrix protein-1) deletion and mice overexpressing hFGF23 displayed widened predentin, decreased alveolar BMD, and enlarged pulp cavity [30, 31]. Although HMWTg mice phenocopy transgenic mice with elevated FGF23, it is likely that there is a direct mineralization inhibitory effect of HMWFGF2 isoforms that are highly expressed in odontoblasts. HMWTg mice uses Col1a1 promoter to drive hHMWFGF2 isoforms overexpression in Col1-rich tissue including osteoblast [10] and odontoblast. HMWFGF2 directly impairs bone mineralization through FGF23-dependent and independent mechanisms [24]. In femurs of HMWTg mice, the expression of bone matrix-related genes including, osteopontin (OPN), matrix gla protein (Mgp), Phex, matrix extracellular phosphoglycoprotein (MEPE), and DMP1 that are involved in the mineralization of bone and teeth were altered with long-term FGF23Ab treatment. OPN mRNA was unchanged with FGF23Ab treatment in HMWTg mice. The expression of Mgp, an inhibitor of mineralization, was increased in HMWTg mice even with FGF23Ab treatment. Additionally, Phex and Mepe mRNA were increased in HMWTg mice and were further increased with FGF23Ab treatment. Furthermore, Dmp1 mRNA levels were decreased in HMWTg mice but was only partially increased with FGF23Ab treatment. Thus, it is evident that HMWFGF2 modulates genes involved in matrix mineralization by both FGF23-dependent and independent mechanisms.

Although it is known that the mineralization defects in XLH arise from defects in FGF23-mediated renal phosphate transport, dietary supplementation of phosphorous and calcium could not sufficiently improve the dentoalveolar hypomineralization in XLH and the Hyp mouse [32]. The dentoalveolar mineralization defects in HMWTg

are accompanied by unaltered serum calcium, decreased serum P_i, and increased PTH. We showed that FGF23Ab markedly reduced the elevated FGF23 in odontoblasts and alveolar bone of HMWTg mandibles that was accompanied by a complete rescue of the dentin hypomineralization and enlarged pulp space and a partial rescue of the osteomalacic alveolar bone. The partial improvement in the alveolar bone morphology is consistent with an increase in serum P_i and a reduction in serum PTH levels in HMWTg with FGF23Ab treatment. Because FGF23Ab monotherapy partially improved the alveolar bone morphology in HMWTg mandibles, it is possible that HMWFGF2 isoforms function independently of FGF23 to inhibit alveolar bone matrix mineralization. 1,25D monotherapy in Hyp mice improved skeletal microarchitecture and bone strength in the absence of phosphate supplementation while enhancing FGF23 expression [23]; however, 1,25D monotherapy was not sufficient to rescue alveolar bone defects in HMWTg mice. FGF23 is known to antagonize renal 1,25D production which in turn, upregulates FGF23 expression in osteocytes [25]. It is possible that FGF23 levels were also increased in response to 1,25D treatment in HMWTg and that could contribute to the observed exacerbation of the alveolar bone morphology. Interestingly, combined 1,25D and FGF23Ab treatment in HMWTg reduces predentin thickness, increases alveolar bone BVF, and decreases pulp chamber area that was comparable to VectorTg mandibles. These observations were accompanied by an elevation in serum calcium and P_i and a decrease in serum PTH to normal levels. These results suggest an additive or synergistic effect of FGF23Ab and 1,25D to promote dentin and alveolar bone mineralization in HMWTg mice.

Our study explored the role of HMWFGF2 on dentoalveolar mineralization. we believe that the minimal sample size in the experiments depicted in Figs. 1 and 2 ($n=3$ and $n=4$, respectively) is a limitation for our study. Furthermore, micro-CT analysis would be a valuable tool to examine the differences in alveolar bone density, pulp chamber size in HMWTg mice with FGF23Ab and/or 1,25D treatments. However, given our limitations, our findings support a novel role for HMWFGF2 in dentin and alveolar bone mineralization in a hypophosphatemic murine model. We showed that dentoalveolar mineralization defects of HMWTg mice in part phenocopies human XLH.

Acknowledgements We thank Amgen Inc., Thousand Oaks, CA for supplying the FGF23 neutralizing antibody. NIH Grant DK098566 and Grant R01 AR072985-05 to MMH supported this project. The content is solely the responsibility of the authors and does not necessarily represent the official views of the National Institutes of Health.

Author Contributions GM contributed to study design, data acquisition, analysis, and interpretation; drafted and critically revised the manuscript. JJ contributed to data acquisition and analysis; and critically revised the manuscript. LX contributed to data acquisition, analysis, and interpretation; and critically revised the manuscript. AV contributed to data acquisition and critically revised the manuscript. MM contributed to study design, data analysis, and interpretation; and critically revised the manuscript. MH contributed to study conception and design, data analysis, and interpretation; and critically revised the manuscript. All authors gave their final approval and agree to be accountable for all aspects of the work.

Declarations

Conflict of interest The authors have no financial relationship with any organization and therefore have nothing to disclose. The authors have full control of all primary data and agree to allow the journal to review the data if requested.

Human and Animal Rights There were no human studies conducted in this manuscript and approval for the animal studies were obtained from The UConn Health Institute of Animal Care and Use Committee.

References

1. Globus RK, Plouet J, Gospodarowicz D (1989) Cultured bovine bone cells synthesize basic fibroblast growth factor and store it in their extracellular matrix. Endocrinology 124(3):1539–1547
2. Hurley MM, Marie PJ, Florkiewicz RZ (2002) Principles of bone biology. Academic Press, San Diego, CA, USA
3. Vidovic-Zdrilic I, Vining KH, Vijaykumar A, Kalajzic I, Mooney DJ, Mina M (2018) Fgf2 enhances odontoblast differentiation by alphasma(+) progenitors in vivo. J Dent Res 97(10):1170–1177
4. Wang JS, Aspenberg P (1996) Basic fibroblast growth factor infused at different times during bone graft incorporation. Titanium chamber study in rats. Acta Orthop Scand 67(3):229–236
5. Arese M, Chen Y, Florkiewicz RZ, Gualandris A, Shen B, Rifkin DB (1999) Nuclear activities of basic fibroblast growth factor: potentiation of low-serum growth mediated by natural or chimeric nuclear localization signals. Mol Biol Cell 10(5):1429–1444
6. Delrieu I (2000) The high molecular weight isoforms of basic fibroblast growth factor (fgf-2): An insight into an intracrine mechanism. FEBS Lett 468(1):6–10
7. Ma X, Dang X, Claus P, Hirst C, Fandrich RR, Jin Y, Grothe C, Kirshenbaum LA, Cattini PA, Kardami E (2007) Chromatin compaction and cell death by high molecular weight fgf-2 depend on its nuclear localization, intracrine erk activation, and engagement of mitochondria. J Cell Physiol 213(3):690–698
8. Touriol C, Bornes S, Bonnal S, Audigier S, Prats H, Prats AC, Vagner S (2003) Generation of protein isoform diversity by alternative initiation of translation at non-aug codons. Biol Cell 95(3–4):169–178
9. Econs MJ, Francis F (1997) Positional cloning of the PEX gene: new insights into the pathophysiology of X-linked hypophosphatemic rickets. Am J Physiol Renal Physiol 273:F489–F498
10. Xiao L, Naganawa T, Lorenzo J, Carpenter TO, Coffin JD, Hurley MM (2010) Nuclear isoforms of fibroblast growth factor 2 are novel inducers of hypophosphatemia via modulation of fgf23 and klotho. J Biol Chem 285(4):2834–284623
11. Bowe AE, Finnegan R, Jan de Beur SM, Cho J, Levine MA, Kumar R, Schiavi SC (2001) Fgf-23 inhibits renal tubular phosphate transport and is a phex substrate. Biochem Biophys Res Commun 284(4):977–981

12. Carpenter TO, Imel EA, Holm IA, Jan de Beur SM, Insogna KL (2011) A clinician's guide to x-linked hypophosphatemia. J Bone Miner Res 26(7):1381–1388
13. Imel EA, Econs MJ (2005) Fibroblast growth factor 23: roles in health and disease. J Am Soc Nephrol 16(9):2565–2575
14. Lee JY, Imel EA (2013) The changing face of hypophosphatemic disorders in the fgf-23 era. Pediatr Endocrinol Rev 10(Suppl 2):367–379
15. Liu S, Tang W, Zhou J, Vierthaler L, Quarles LD (2007) Distinct roles for intrinsic osteocyte abnormalities and systemic factors in regulation of fgf23 and bone mineralization in hyp mice. Am J Physiol Endocrinol Metab 293(6):E1636-1644
16. Martin A, David V, Quarles LD (2012) Regulation and function of the fgf23/klotho endocrine pathways. Physiol Rev 92(1):131–15526
17. Souza MA, Soares Junior LA, Santos MA, Vaisbich MH (2010) Dental abnormalities and oral health in patients with hypophosphatemic rickets. Clinics (Sao Paulo) 65(10):1023–1026
18. Ribeiro TR, Costa FW, Soares EC, Williams JR Jr, Fonteles CS (2015) Enamel and dentin mineralization in familial hypophosphatemic rickets: a micro-ct study. Dentomaxillofac Radiol 44(5):20140347
19. Chaussain-Miller C, Sinding C, Wolikow M, Lasfargues J, Godeau G, Garabédian M (2003) Dental abnormalities in patients with familial hypophosphatemic vitamin D-resistant rickets: prevention by early treatment with 1-hydroxyvitamin D. J Pediatr. 142(3):324–31
20. Boukpessi T, Septier D, Bagga S, Garabedian M, Goldberg M, Chaussain-Miller C (2006) Dentin alteration of deciduous teeth in human hypophosphatemic rickets. Calcif Tissue Int 79(5):294–300
21. Opsahi S, Gaucher C, Bardet C, Rowe PS, George A, Linglart A, Chaussain C (2012) Tooth dentin defects reflect genetic disorders affecting bone mineralization. Bone 50(4):989–997
22. Aono Y, Yamazaki Y, Yasutake J, Kawata T, Hasegawa H, Urakawa I, Fujita T, Wada M, Yamashita T, Fukumoto S et al (2009) Therapeutic effects of anti-FGF23 antibodies in hypophosphatemic rickets/osteomalacia. J Bone Miner Res 24(11):1879–1888
23. Liu ES, Martins JS, Raimann A, Chae BT, Brooks DJ, Jorgetti V, Bouxsein ML, Demay MB (2016) 1,25-dihydroxyvitamin d alone improves skeletal growth, microarchitecture, and strength in a murine model of xlh, despite enhanced fgf23 expression. J Bone Miner Res 31(5):929–939
24. Xiao L, Homer-Bouthiette C, Hurley MM (2018) Fgf23 neutralizing antibody partially improves bone mineralization defect of hmwfgf2 isoforms in transgenic female mice. J Bone Miner Res 33(7):1347–1361
25. Foster BL, Nociti FH Jr, Somerman MJ (2014) The rachitic tooth. Endocr Rev 35(1):1–34
26. Abe K, Ooshima T, Masatomi Y, Sobue S, Moriwaki Y (1989) Microscopic and crystallographic examinations of the teeth of the x-linked hypophosphatemic mouse. J Dent Res 68(11):1519–1524
27. Fong H, Chu EY, Tompkins KA, Foster BL, Sitara D, Lanske B, Somerman MJ (2009) Aberrant cementum phenotype associated with the hypophosphatemic hyp mouse. J Periodontol 80(8):1348–1354
28. Du E, Xiao L, Hurley MM (2017) FGF23 Neutralizing Antibody Ameliorates Hypophosphatemia and Impaired FGF Receptor Signaling in Kidneys of HMWFGF2 Transgenic Mice. J Cell Physiol 232(3):610–616
29. Xiao Z, Huang J, Cao L, Liang Y, Han X, et al. (2014) Osteocyte-Specific Deletion of Fgfr1 Suppresses FGF23. PLoS ONE. 9(8):e104154.
30. Chen L, Liu H, Sun W, Bai X, Karaplis AC, Goltzman D, Miao D (2011) Fibroblast growth factor 23 overexpression impacts negatively on dentin mineralization and dentinogenesis in mice. Clin Exp Pharmacol Physiol 38(6):395–402
31. Ye L, MacDougall M, Zhang S, Xie Y, Zhang J, Li Z, Lu Y, Mishina Y, Feng JQ (2004) Deletion of dentin matrix protein-1 leads to a partial failure of maturation of predentin into dentin, hypomineralization, and expanded cavities of pulp and root canal during postnatal tooth development. J Biol Chem 279(18):19141–19148
32. Masatomi Y, Nakagawa Y, Kanamoto Y, Sobue S, Ooshima T (1996) Effects of serum phosphate level on formation of incisor dentine in hypophosphatemic mice. J Oral Pathol Med 25(4):182–187